



The Hidden "Agn Main Sequence": Evidence for a Universal Black Hole Accretion to Star Formation Rate Ratio Since $z \approx 2$ Producing an $M_{BH}-M_*$ Relation

J. R. Mullaney, Emanuele Daddi, M. Béthermin, D. Elbaz, S. Juneau, M. Pannella, M. T. Sargent, D. M. Alexander, R. C. Hickox

► To cite this version:

J. R. Mullaney, Emanuele Daddi, M. Béthermin, D. Elbaz, S. Juneau, et al.. The Hidden "Agn Main Sequence": Evidence for a Universal Black Hole Accretion to Star Formation Rate Ratio Since $z \approx 2$ Producing an $M_{BH}-M_*$ Relation. The Astrophysical journal letters, 2012, 753, pp.L30. 10.1088/2041-8205/753/2/L30 . cea-00832927

HAL Id: cea-00832927

<https://cea.hal.science/cea-00832927>

Submitted on 5 Jan 2021

HAL is a multi-disciplinary open access archive for the deposit and dissemination of scientific research documents, whether they are published or not. The documents may come from teaching and research institutions in France or abroad, or from public or private research centers.

L'archive ouverte pluridisciplinaire **HAL**, est destinée au dépôt et à la diffusion de documents scientifiques de niveau recherche, publiés ou non, émanant des établissements d'enseignement et de recherche français ou étrangers, des laboratoires publics ou privés.

THE HIDDEN “AGN MAIN SEQUENCE”: EVIDENCE FOR A UNIVERSAL BLACK HOLE ACCRETION TO STAR FORMATION RATE RATIO SINCE $z \sim 2$ PRODUCING A $M_{\text{BH}}-M_*$ RELATION

J. R. MULLANEY^{1,2}, E. DADDI¹, M. BÉTHÉRMIN¹, D. ELBAZ¹, S. JUNEAU¹, M. PANNELLA¹, M. T. SARGENT¹, D. M. ALEXANDER², R. C. HICKOX³

Draft version October 16, 2018

ABSTRACT

Using X-ray stacking analyses we estimate the average amounts of supermassive black hole (SMBH) growth taking place in star-forming galaxies (SFGs) at $z \sim 1$ and $z \sim 2$ as a function of galaxy stellar mass (M_*). We find the average SMBH growth rate follows remarkably similar trends with M_* and redshift as the average star-formation rates (SFRs) of their host galaxies (i.e., $\dot{M}_{\text{BH}} \propto M_*^{0.86 \pm 0.39}$ for the $z \sim 1$ sample and $\dot{M}_{\text{BH}} \propto M_*^{1.05 \pm 0.36}$ for the $z \sim 2$ sample). It follows that the ratio of SMBH growth rate to SFR is (a) flat with respect to M_* (b) not evolving with redshift and (c) close to the ratio required to maintain/establish a SMBH to M_* ratio of $\approx 10^{-3}$ as also inferred from today’s $M_{\text{BH}}-M_{\text{Bulge}}$ relationship. We interpret this as evidence that SMBHs have, on average, grown in-step with their host galaxies since at least $z \sim 2$, irrespective of host galaxy mass and AGN triggering mechanism. As such, we suggest that the same secular processes that drive the bulk of star formation are also responsible for the majority of SMBH growth. From this, we speculate that it is the availability of gas reservoirs that regulate both cosmological SMBH growth and star formation.

Subject headings: galaxies: active—galaxies: evolution—galaxies: star formation—X-rays: general

1. INTRODUCTION

The tight observed relationship between galaxy bulge mass and the mass of its central, supermassive black hole (SMBH; e.g., Häring & Rix 2004), hereafter $M_{\text{BH}}-M_{\text{Bulge}}$, suggests galaxy growth (i.e., star-formation) is closely tied to the principal mode of SMBH growth: accretion during periods of nuclear activity (i.e., active galactic nuclei, or AGN). However, the $M_{\text{BH}}-M_{\text{Bulge}}$ relationship only provides a snapshot of the end result, with the details surrounding when, how and under what conditions these links were forged remaining poorly understood. Indeed, it is not yet clear whether *all* episodes of star-formation are eventually accompanied by SMBH growth, or whether such evolutionary links are limited to the most rapidly growing systems, such as those induced by major-mergers (see Alexander & Hickox 2011 for a review). A major difficulty in exploring the links between ongoing SMBH and galaxy growth stems partly from scatter introduced by the different duty cycles of AGN and star-formation episodes, leading to what appears to be only very weak correlations between the two events (e.g., Silverman et al. 2009; Mullaney et al. 2012).

Since SMBH growth appears to be so closely tied to galaxy growth, it is pertinent to ask whether average SMBH accretion rates trace star-formation rates (SFRs). In this vein, Daddi et al. (2007b) showed that the ratio of average SMBH accretion rate to SFR in star-forming galaxies (SFGs) at $z \sim 2$ was roughly consistent with that inferred from today’s $M_{\text{BH}}-M_{\text{Bulge}}$ relationship. However, focussing on only the global average conceals details of how SMBH and galaxy mass is built

up. Indeed, it is now evident that SFGs have formed stars at a rate that is roughly proportional to their stellar masses (M_*) since at least $z \sim 2$, while their average specific SFRs (i.e., $\text{sSFR} = \text{SFR}/M_*$) increase strongly with redshift (e.g., Noeske et al. 2007; Elbaz et al. 2007; Daddi et al. 2007a; Pannella et al. 2009; Karim et al. 2011; Elbaz et al. 2011). Here, we determine whether these trends between SFR, M_* and redshift for SFGs also extend to the growth of their resident SMBHs. We use $H_0 = 71 \text{ km s}^{-1} \text{ Mpc}^{-1}$, $\Omega_\Lambda = 0.73$, $\Omega_M = 0.27$ and a Chabrier initial mass function.

2. DATA AND ANALYSES

We measure the average SMBH accretion rates in SFGs at $0.5 < z < 2.5$ in the GOODS-South field. Our two samples of $z \sim 1$ and $z \sim 2$ galaxies (607 and 1146 sources, respectively) are from the K-selected catalogue of Daddi et al. (2007a; 2007b; see also Salimi et al. 2012 for details of the $z \sim 1$ sample). SFRs for these galaxies are based on 24 μm and UV observations, respectively, and are known to be unbiased on average (Daddi et al. 2007a; Elbaz et al. 2010). Both samples were divided into the same set of stellar mass (M_*) bins. The average SFR of SFGs in these bins, plotted as a function of M_* , is shown in Fig. 1a. The shallower slope of the $z \sim 1$ SFR- M_* relation compared to the $z \sim 2$ sample is due to an Eddington bias introduced by the flux limit of the 24 μm data used to estimate their SFRs. By comparing like-for-like average X-ray emission (and inferred SMBH accretion rates) with average SFRs and using the SFGs as priors for our X-ray matching/stacking we ensure that this bias has no effect on our results.

The X-ray data used for this study were taken from the 4 Ms *Chandra* deep-field observations (Cycle 9 DDT; see Xue et al. 2011 for details), which entirely cover our SFG samples. To determine the average level of SMBH accretion taking place in the SFGs we account for X-ray

¹ Irfu/Service d’Astrophysique, CEA-Saclay, Orme des Merisiers, 91191, Gif-sur-Yvette Cedex, France

² Department of Physics, Durham University, South Road, Durham DH1 3LE, U.K.

³ Department of Physics and Astronomy, Dartmouth College, 6127 Wilder Laboratory, Hanover, NH 03755, USA

TABLE 1
DERIVED AVERAGE PHYSICAL PROPERTIES OF SUB-SAMPLES

(1)	(2)	(3)	(4)	(5)	(6)	(7)	(8)	(9)
Mass range	N_{Det}	N_{Stk}	$\langle M_* \rangle$	$\langle \text{SFR} \rangle$	$\langle F_{2-10\text{keV}} \rangle$	$\langle L_{2-10\text{keV}} \rangle$	$\langle L_{\text{Bol}} \rangle$	$\langle \dot{M}_{\text{BH}} \rangle$
$z \sim 1$								
9.76 – 10.09	12	138	9.952 ± 0.088	3.89 ± 0.32	20^{+38}_{-16}	$0.5^{+1.0}_{-0.3}$	$3.3^{+5.8}_{-2.1}$	$2.0^{+3.6}_{-1.3}$
10.09 – 10.42	22	112	10.232 ± 0.092	7.19 ± 0.51	22^{+15}_{-10}	$0.71^{+0.94}_{-0.37}$	$4.4^{+5.3}_{-2.4}$	$2.7^{+3.2}_{-1.5}$
10.42 – 10.75	28	82	10.592 ± 0.098	12.62 ± 0.97	82^{+43}_{-31}	$3.8^{+2.9}_{-1.6}$	22^{+17}_{-10}	14^{+10}_{-6}
10.75 – 11.25	41	77	10.95 ± 0.14	16.0 ± 1.6	82^{+48}_{-33}	$3.7^{+2.5}_{-1.4}$	22^{+14}_{-8}	$13.3^{+8.5}_{-5.2}$
$z \sim 2$								
9.76 – 10.09	20	327	9.907 ± 0.094	20.77 ± 0.89	$9.9^{+7.6}_{-5.1}$	$2.8^{+2.8}_{-1.3}$	17^{+16}_{-8}	$10.3^{+9.6}_{-5.0}$
10.09 – 10.42	32	206	10.24 ± 0.10	34.1 ± 2.0	$17.3^{+7.2}_{-5.6}$	$4.0^{+2.9}_{-1.5}$	24^{+16}_{-10}	$14.7^{+9.7}_{-5.8}$
10.42 – 10.75	34	67	10.564 ± 0.091	58.4 ± 5.3	50^{+24}_{-18}	$12.9^{+8.8}_{-4.9}$	77^{+49}_{-30}	47^{+30}_{-18}
10.75 – 11.25	18	28	10.90 ± 0.11	151 ± 22	140^{+130}_{-80}	25^{+25}_{-12}	150^{+140}_{-70}	90^{+86}_{-44}

NOTE. — (1) Stellar mass range ($\log[M_\odot]$), (2) Number of X-ray detected galaxies, (3) Number of stacked X-ray undetected galaxies, (4) Stellar mass ($\log[M_\odot]$), (5) SFR ($M_\odot \text{ yr}^{-1}$), (6) Observed-frame 2-10 keV X-ray flux ($10^{-17} \text{ ergs s}^{-1} \text{ cm}^{-2}$), (7) Intrinsic AGN rest-frame 2-10 keV X-ray luminosity ($10^{42} \text{ ergs s}^{-1} \text{ cm}^{-2}$) (8) Bolometric AGN luminosity ($10^9 L_\odot$), (9) SMBH accretion rate ($10^{-3} M_\odot \text{ yr}^{-1}$). Columns 4-9 contain mean-average values.

non-detections as well as X-ray detections. First, we used positional matching to identify those galaxies detected in X-rays, matching to the optical positions reported in Xue et al. (2011) and assuming a matching radius of $1''$. The numbers of identified matches in each of our M_* and redshift bins are given in Table 1. For the remainder, we stacked the X-ray data at the optical positions of the SFGs, taking care to avoid detected sources and only stacking within $8'$ of the average aim-point of the *Chandra* observations.⁴ For each of our redshift and mass bins the total (i.e., detected + undetected) X-ray counts are dominated by the X-ray detected sources. Average count rates were determined by summing the counts from the detected sources and the stacks then dividing this by the total effective exposure times (of both detected and undetected sources). Average band ratios, fluxes at the observed-frame 2-10 keV band and obscuration-corrected luminosities at a rest-frame 2-10 keV band (i.e., L_X) were calculated using the methodology outlined in Luo et al. (2008) which uses band-ratios to correct for obscuration (see our Table 1). The average contribution to L_X from star-formation was calculated using two different SFR- L_X relations (from Ranalli et al. 2003 and Vattakunnel et al. 2012) and subtracted to leave the intrinsic L_X of the AGN. Both relations estimate a non-AGN contribution of $< 5\%$ in each of our mass and redshift bins, meaning this correction has no significant impact on our results.

Once the average intrinsic X-ray luminosities had been estimated for the SFGs in each of our M_* and redshift bins, we used this information to estimate average AGN bolometric luminosities (i.e., L_{Bol}). For simplicity, we derive our main results using a constant bolometric correction factor of 22.4 to convert L_X to L_{Bol} (the median bolometric correction factor of a sample of local, $L_X = 10^{41-46} \text{ ergs s}^{-1}$ AGN from Vasudevan & Fabian 2007). From L_{Bol} we derive SMBH accretion rates (i.e., \dot{M}_{BH}) using:

$$\dot{M}_{\text{BH}}(M_*, z) = \frac{(1 - \epsilon)L_{\text{bol}}(M_*, z)}{\epsilon c^2} \quad (1)$$

where c is the speed of light in a vacuum and ϵ is the efficiency by which mass is converted into radiated energy via the accretion process. Here we assume $\epsilon = 0.1$ (e.g., Marconi et al. 2004), or that roughly 10% of mass within the accreting system is converted into energy that is radiated away via electromagnetic radiation, irrespective of M_{BH} .

As the number of X-ray counts for each bin is dominated (i.e., $> 80\%$) by X-ray detected sources, uncertainties on the mean L_X were calculated using a bootstrapping technique; repeatedly selecting 2/3 of the detected sample in each bin at random and calculating the dispersion of the resulting L_X distribution. The uncertainties on L_{Bol} and \dot{M}_{BH} were then propagated from our estimates of the uncertainties on the mean L_X .

3. RESULTS

In Fig. 1b we plot the average L_X of X-ray detected + undetected (i.e., stacked) SFGs as a function of M_* for our two redshift samples. Both our $z \sim 1$ and $z \sim 2$ samples show a clear increase in their average L_X with increasing M_* for the mass range considered. This is in contrast to studies of individually detected X-ray AGN which find no such correlation (e.g., Mullaney et al. 2012). It is only when the scatter in L_X due to AGN variability is averaged-out that the correlation between L_X and M_* for SFGs presents itself. A least-squares fit to these data gives $L_X \propto M_*^{0.86 \pm 0.39}$ for the $z \sim 1$ sample and $L_X \propto M_*^{1.05 \pm 0.36}$ for the $z \sim 2$ sample. As we neglect the (unknown) possible variations of accretion efficiencies and bolometric corrections with stellar masses, L_X can be directly replaced by \dot{M}_{BH} in these equations to give the same relationships between \dot{M}_{BH} and M_* . Importantly, we also find that the average L_X of SFGs increases with redshift, being a factor of 5.2 ± 1.4 higher, on average, at $z \sim 2$ compared to $z \sim 1$. This is comparable to the factor of 6.1 ± 2.3 higher average SFRs of the $z \sim 2$ sample.

To demonstrate this last point we have included in our L_X - M_* plot (Fig. 1b) the observed trend between

⁴ We note the results from our X-ray stacks are consistent within the errors of those obtained using CSTACK (<http://cstack.ucsd.edu/>) developed by Takamitsu Miyaji, which uses the 2 Ms CDF-S data.

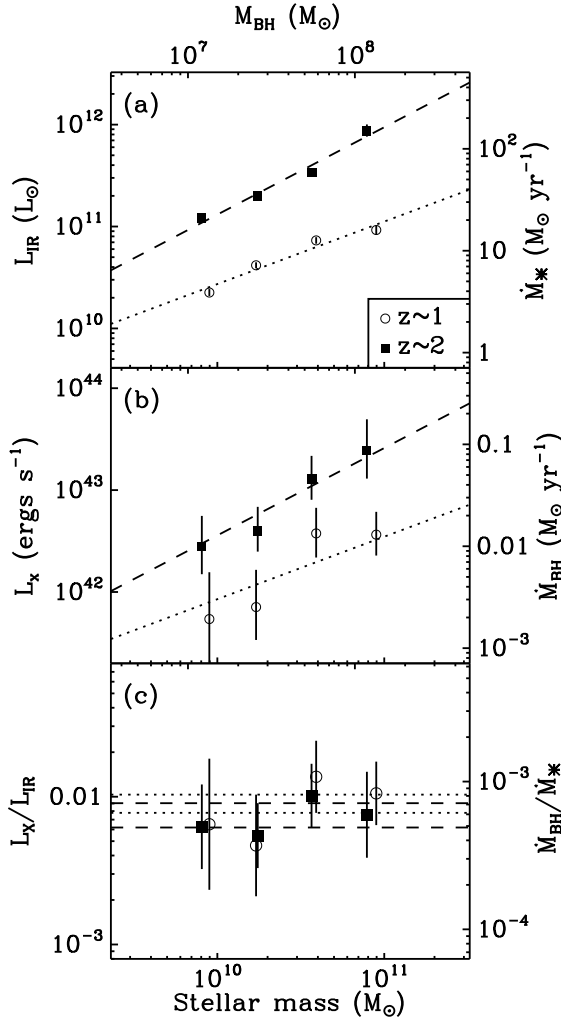


FIG. 1.— (a) Average SFRs (right-hand axis) versus stellar mass for our $z \sim 1$ (open circles) and $z \sim 2$ (filled squares) samples of SFGs (left-hand axis gives equivalent infrared luminosity for illustrative purposes only). Dotted and dashed lines indicate a least-squares linear fit to these data. (b) Average X-ray luminosities of the SFGs in our samples (same symbols as top panel) after accounting for any host galaxy contribution. Lines have the same gradients as in the top panel, only normalised to best-fit the inferred \dot{M}_{BH} , which is indicated in the right-hand axis. (c) Average SMBH accretion rate to SFR ratio for our two redshift samples. The uncertainties on these points are consistent with a flat $\dot{M}_{\text{BH}}/\text{SFR}$ ratio with respect to M_* for both the $z \sim 1$ and $z \sim 2$ samples, indicated by the dotted and dashed lines, respectively. $1\text{-}\sigma$ uncertainties are included in each panel, but are smaller than the points in panel (a).

SFR and M_* derived from our two samples of SFGs (i.e., $\text{SFR} \propto M_*^{0.6}$ and $\text{SFR} \propto M_*^{0.9}$ for the $z \sim 1$ and $z \sim 2$ populations, respectively), normalised to fit the average inferred \dot{M}_{BH} of the respective redshift sample but maintaining the gradient. Plotting $\dot{M}_{\text{BH}}/\text{SFR}$ as a function of M_* (Fig. 1c) we find this ratio is only marginally dependent on M_* and is strikingly similar for our $z \sim 1$ and $z \sim 2$ samples (i.e., $\dot{M}_{\text{BH}}/\text{SFR} \propto M_*^{0.3 \pm 0.4}$ and $\dot{M}_{\text{BH}}/\text{SFR} \propto M_*^{0.2 \pm 0.4}$ for the $z \sim 1$ and $z \sim 2$ samples, respectively). Furthermore, the uncertainties are consistent with a flat $\dot{M}_{\text{BH}}/\text{SFR}$ ratio with respect to M_* for both samples (i.e., $\dot{M}_{\text{BH}} = [0.6 - 0.8] \times 10^{-3} \cdot \text{SFR}$ for our $z \sim 1$ sample and $\dot{M}_{\text{BH}} = [0.5 - 0.7] \times 10^{-3} \cdot \text{SFR}$ for

our $z \sim 2$ sample).⁵

By taking the average X-ray output of SFGs it follows that the ensemble growth rate of SMBHs increases with both increasing M_* and redshift in a manner that is remarkably similar to the average levels of star-formation taking place in SFGs. The independence of the average $\dot{M}_{\text{BH}}/\text{SFR}$ ratio on M_* implies its constancy during the rapid growth phases of galaxies. Next, we consider how this constant ratio conforms to our understanding of relative SMBH growth both locally and at high redshifts.

The mass of a SMBH today, at redshift $z_f = 0$, can be described in terms of its total accretion history since z_i and its mass at z_i , i.e.,⁶

$$M_{\text{BH}}(z_f) = M_{\text{BH}}(z_i) + \int_{z=z_i}^{z=z_f} \dot{M}_{\text{BH}}(t) dt \quad (2)$$

Our observations support a constant average ratio between the SMBH and galaxy growth rates, i.e., $\dot{M}_{\text{BH}} = \alpha \dot{M}_*$.⁷ Replacing the resulting integral with $\Delta M_*(z = z_i \rightarrow z_f)$, we obtain,

$$M_{\text{BH}}(z_f) = M_{\text{BH}}(z_i) + \alpha \Delta M_*(z = z_i \rightarrow z_f) \quad (3)$$

Similarly, the stellar mass of the host galaxy at z_f is given by,

$$M_*(z_f) = M_*(z_i) + \Delta M_*(z = z_i \rightarrow z_f) \quad (4)$$

so the black hole to stellar mass ratio is given by,

$$\frac{M_{\text{BH}}(z_f)}{M_*(z_f)} = \frac{M_{\text{BH}}(z_i) + \alpha \Delta M_*(z = z_i \rightarrow z_f)}{M_*(z_i) + \Delta M_*(z = z_i \rightarrow z_f)} \quad (5)$$

Defining β as the initial M_{BH} to M_* ratio (relative to the growth rate ratio, i.e., α) and γ as the relative change in M_* , i.e.,

$$M_{\text{BH}}(z_i) = \beta \alpha M_*(z_i), \quad \gamma = \frac{\Delta M_*(z = z_i \rightarrow z_f)}{M_*(z_i)} \quad (6)$$

we obtain,

$$\frac{M_{\text{BH}}(z_f)}{M_*(z_f)} = \alpha \frac{\gamma + \beta}{\gamma + 1} \approx \alpha \quad (\text{when } \gamma \gg \beta) \quad (7)$$

Thus, as soon as enough activity has taken place so that the (uncertain) initial conditions can be neglected, one expects constant M_{BH} to M_* ratios independent of redshift and roughly equal to the observed growth rate ratio. It is not surprising then that the growth ratios are close to the SMBH to stellar mass ratio inferred from today's $M_{\text{BH}}-M_{\text{Bulge}}$ relationship, indicating that this relative growth rate is crucial in defining these ratios.

4. DISCUSSION: A HIDDEN AGN “MAIN SEQUENCE”

Our results suggest that it is coeval growth at constant relative rates averaged over cosmological timescales that

⁵ Adopting a luminosity-dependent bolometric correction factor from Hopkins et al. (2007) gives $M_{\text{BH}}/\text{SFR} \propto M_*^{0.5 \pm 0.5}$ for both redshift bins; the error-bars remain consistent with a flat distribution.

⁶ We neglect merging SMBHs as they will not affect the total mass contained within SMBHs while merger-induced starbursts contribute only $\sim 10\%$ of stellar-mass build-up (Rodighiero et al. 2011).

⁷ Note: $\dot{M}_* \equiv \text{SFR}$

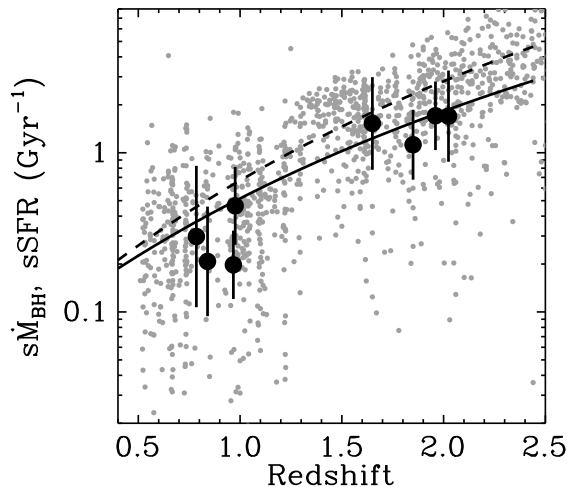


FIG. 2.— Specific SMBH accretion rates (i.e., $s\dot{M}_{\text{BH}} = \dot{M}_{\text{BH}}/M_{\text{BH}}$; assuming $M_{\text{BH}} = 1.5 \times 10^{-3} M_*$) plotted as a function of redshift for our stellar mass and redshift bins (large black points). Included in this plot are the sSFRs of the galaxies in our samples (small gray points), and the sSFR- z relationships from Elbaz et al. (2011) and Pannella et al. (2009) (solid and dashed lines, respectively). We have increased the specific SMBH accretion rates by a factor of 2 to account for missing AGN due to e.g. obscuration, but note that the *relative* change in average $\dot{M}_{\text{BH}}/M_{\text{BH}}$ between our redshift bins is remarkably similar to that of the sSFRs.

produces the links between SMBH and stellar mass inferred from the $M_{\text{BH}}-M_{\text{Bulge}}$ relation. To address this in more detail there are a number of points that should be considered carefully.

First, we emphasise that our results are cosmologically relevant, referring to the bulk of the SMBH and galaxy growth. The $0.5 < z < 2.5$ epoch spanned by our samples correspond to the vast majority of both global star (e.g., Dickinson et al. 2003; Magnelli et al. 2011) and SMBH (e.g., Marconi et al. 2004) formation history.

Likewise, although we miss the most luminous AGN their absence will not change our results. Integrating the “LADE” AGN X-ray luminosity function of Aird et al. 2010, we estimate that ~ 20 – 30% of all SMBH accretion at $0.5 < z < 2.5$ takes place in AGNs that are rare enough such that ≤ 3 would be expected to be found in our survey (i.e., rarer than three per $2 \times 10^5 \text{ Mpc}^3$ at $z \sim 1$ and three per $4 \times 10^5 \text{ Mpc}^3$ at $z \sim 2$, corresponding to $L_X > 2 \times 10^{44} \text{ ergs s}^{-1}$ and $L_X > 3 \times 10^{44} \text{ ergs s}^{-1}$, respectively). Similarly, we could miss $\lesssim 2\%$ of the SFR density because of volume effects. We note that the fraction of AGNs in low-SFR galaxies not included in our SFG sample is also negligible at these redshifts, being $\lesssim 10\%$ (e.g., Mullaney et al. 2012).

Obscuration is a potentially more serious issue, as we will underestimate the contribution of the heavily obscured (i.e., Compton-thick) AGNs thought to be responsible for $\lesssim 50\%$ of total SMBH growth (e.g., Gilli et al. 2007). This could introduce a factor of $\lesssim 2$ correction, but is unlikely to be substantially larger than the observed, unobscured contribution. Obscuration due to orientation effects (unified model) is unlikely to depend strongly on either mass or redshift and, as such, will not affect the observed correlations. It is unclear whether the levels of obscuration due to merger driven starbursts changes as a function of galaxy mass and/or redshift.

However, the fraction of starbursts does not appear to change significantly with redshift or galaxy mass and accounts for only 10–15% of all star-formation (at least for the ranges considered here; Rodighiero et al. 2011; Sargent et al. 2012).

This obscured AGN fraction, together with the fact that a fraction of the stars forming will quickly die due to stellar evolution, leads us to conclude that our results support a constant M_{BH} to M_* ratio of:

$$\frac{M_{\text{BH}}}{M_*} \approx (1 - 2) \times 10^{-3} \quad (8)$$

at $0.5 < z < 2.5$ – consistent with the conclusions of Jahnke et al. (2009) and Cisternas et al. (2011a). This ratio is also consistent with the local $M_{\text{BH}}/M_{\text{Bulge}}$ ratio, suggesting that it is the same relation. At this point it is important to note that, while there is some evidence to suggest that today’s M_{BH} correlates most tightly with bulge mass (Kormendy et al. 2011), for the sake of this letter we do not distinguish between galaxy and bulge mass/SFR as it is impossible to reliably determine which of the stars formed at $z \gtrsim 0.5$ will be in bulges by $z \sim 0$. Having said that, it is thought the the majority of stars formed at these high redshifts in the M_* range considered will collapse to form massive bulges by $z \sim 0$ (e.g., Renzini 2006), probably due to the effects of mergers.

Using Eqn. (8) we can compute approximate SMBH masses for our galaxy samples. Since the \dot{M}_{BH} to SFR ratio has remained consistent with the SMBH and galaxy mass ratio since $z \sim 2$ the specific SMBH growth rate (i.e., $s\dot{M}_{\text{BH}} = \dot{M}_{\text{BH}}/M_{\text{BH}}$) traces the same trend with redshift as the average sSFRs of SFGs (e.g., Pannella et al. 2009; Elbaz et al. 2011; Fig. 2). Thus, when doing ensemble (i.e., time) averages, the SMBH population forms an “AGN main-sequence” (where roughly $\dot{M}_{\text{BH}} \propto M_{\text{BH}}$, on average) that follows the same trends with stellar mass and redshift as the so-called galactic main sequence of e.g., Noeske et al. (2007); Elbaz et al. (2007); Daddi et al. (2007a).

It is interesting to interpret these results in terms of the frequency of nuclear and star-forming activity in galaxies. For this, we consider the distribution of AGN Eddington ratios ($\lambda_e \propto \dot{M}_{\text{BH}}/M_{\text{BH}}$) and galaxy sSFRs. Recently, Aird et al. (2012) suggested that the λ_e distribution of X-ray AGNs can be described purely as a function of λ_e and redshift; i.e., independently of M_* (Fig. 3a).⁸ This broad distribution for AGNs, which spans over four orders of magnitude in λ_e (see also, e.g., Babić et al. 2007; Hopkins & Hernquist 2009), contrasts with the distribution of sSFR of galaxies that is remarkably narrow, yet also independent of M_* (Sargent et al. 2012; Fig. 3a). This is the main reason why the AGN main sequence remains hidden; there are strong changes in $s\dot{M}_{\text{BH}}$ compared to minor changes in the sSFRs of galaxies (Fig. 3). This has the implication that outliers should exist in the $M_{\text{BH}}-M_*$ relation when the SMBH growth has taken advantage over the M_* growth and vice versa, in qualita-

⁸ Studies of optically-selected, broad-line quasars have reported log-normal λ_e distributions. However, by selection, those AGNs have considerably higher average L_{Bol} ($\approx 10^{13} L_{\odot}$; e.g., Shen et al. 2008) than our samples and, as such, are less directly relevant to our analyses.

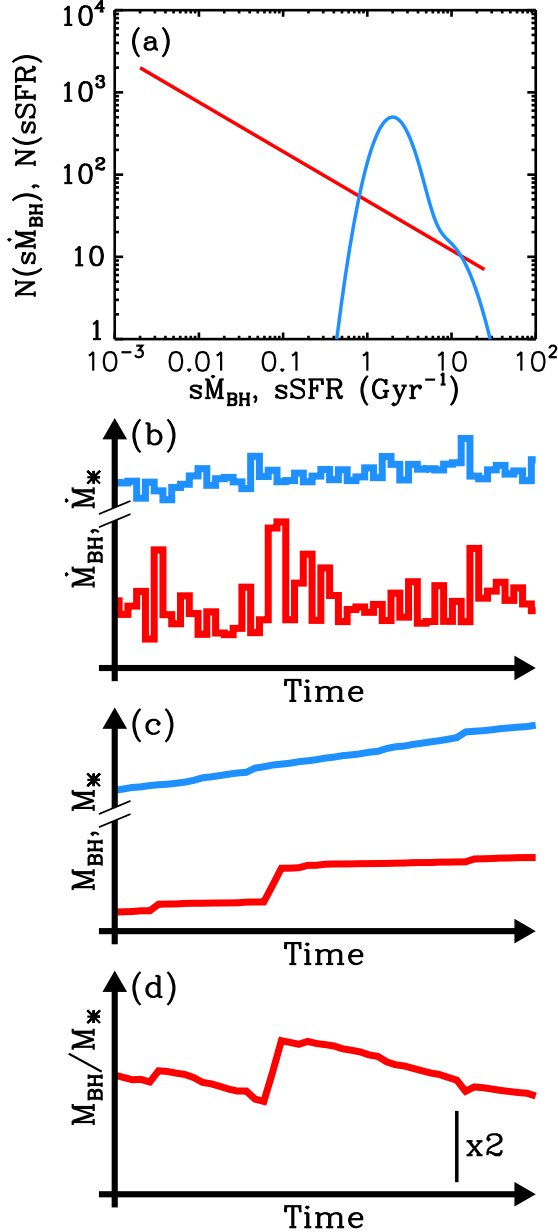


FIG. 3.— (a): Probability distribution functions (PDFs) of $s\dot{M}_{\text{BH}}$ (\propto Eddington ratio; red; Aird et al. 2012) and $s\text{SFR}$ (blue; Sargent et al. 2012) at a given redshift (arbitrary y -scaling). Note the broad $s\dot{M}_{\text{BH}}$ PDF, indicative of the large variations in nuclear activity compared to the $s\text{SFR}$ of the host. *Lower three panels:* Cartoon illustrating the growth rates (b) and total and relative masses (c and d, respectively) of SMBHs and their hosts. The host grows steadily, whereas the SMBH grows in fits and spurts, causing the SMBH mass to “lead and lag” the galaxy mass at different times but, on average, remaining closely tied. Scale in panel (d) indicates a factor of 2 change.

tive agreement with observations (e.g., Alexander et al. 2008; Targett et al. 2012; also Volonteri & Stark 2011).

The rise of the specific growth of galaxies with redshift has recently been attributed to the strong increase in the gas fractions of galaxies from $z = 0$ to 2 (Daddi et al. 2008, 2010; Tacconi et al. 2010; Geach et al. 2011). Given that the cosmological growth rate between SMBHs and M_* remains roughly constant, it seems that gas fractions also play an important role in driving SMBH growth during this epoch. However, clarifying the physical processes (feedback, volume effects, etc.) that set $\dot{M}_{\text{BH}}/\text{SFR} \approx 10^{-3}$ and determine how gas fraction translates to different $s\text{SFR}$ and $s\dot{M}_{\text{BH}}$ distributions (Fig. 3a) remains an open issue that is beyond the scope of this letter.

Our results provide insights into how the relationships between SMBHs and their host galaxies are forged. The vast majority (i.e., $\approx 98\%$) of galaxies that form our parent sample are main-sequence (MS) SFGs (e.g., Rodighiero et al. 2011). Morphological and dynamical studies do find evidence of mergers among these galaxies (e.g., Elmegreen et al. 2007; Förster Schreiber et al. 2009), but being on the MS (Kartaltepe et al. 2011) implies their star-formation is not strongly enhanced by these interactions (Di Matteo et al. 2008). Such MS galaxies are responsible for $\approx 90\%$ (Elbaz et al. 2011; Rodighiero et al. 2011; Sargent et al. 2012) of all star-formation taking place during this epoch. Of course, the most massive, distant galaxies and SMBHs probed here will have grown their mass at earlier times when other processes – such as major-mergers – may have played a more dominant role. However, for SFGs to have $\langle \frac{\dot{M}_{\text{BH}}}{\text{SFR}} \rangle \approx \frac{\dot{M}_{\text{BH}}}{M_*}|_{z=0}$ during the time when the bulk of today’s stellar and SMBH mass was built-up implies that a significant fraction of all SMBH growth takes place in MS galaxies whose SFRs are not enhanced by mergers. This view is consistent with recent studies of the $s\text{SFR}$ s and morphologies of X-ray selected AGN hosts which find that the AGN population is dominated by non-mergers (e.g., Cisternas et al. 2011b; Schawinski et al. 2011; Mullaney et al. 2012; Kocevski et al. 2012; Santini et al. 2012). Indeed, results from recent hydrodynamical models (e.g., Bournaud et al. 2011) suggest that it is possible to have efficient SMBH accretion inside gas rich, high redshift clumpy galaxies, without invoking galaxy-galaxy interactions or mergers.

We thank M. Dickinson, R. Gilli, A. Renzini and the anonymous referee. We acknowledge financial support from STFC (DMA) and grants: ERC-StG UPGAL 240039, ANR-08-JCJC-0008.

REFERENCES

- Aird, J., Nandra, K., Laird, E. S., et al. 2010, MNRAS, 401, 2531
Aird, J., Coil, A. L., Moustakas, J., et al. 2012, ApJ, 746, 90
Alexander, D. M., & Hickox, R. C. 2011, arXiv:1112.1949
Alexander, D. M., Brandt, W. N., Smail, I., et al. 2008, AJ, 135, 1968
Babić, A., Miller, L., Jarvis, M. J., et al. 2007, A&A, 474, 755
Bournaud, F., Dekel, A., Teyssier, R., et al. 2011, ApJ, 741, L33
Cisternas, M., Jahnke, K., Bongiorno, A., et al. 2011a, ApJ, 741, L11
Cisternas, M., Jahnke, K., Inskip, K. J., et al. 2011b, ApJ, 726, 57
Daddi, E., Dannerbauer, H., Elbaz, D., et al. 2008, ApJ, 673, L21
Daddi, E., Dickinson, M., Morrison, G., et al. 2007a, ApJ, 670, 156
Daddi, E., Alexander, D. M., Dickinson, M., et al. 2007b, ApJ, 670, 173
Daddi, E., Bournaud, F., Walter, F., et al. 2010, ApJ, 713, 686
Di Matteo, P., Bournaud, F., Martig, M., et al. 2008, A&A, 492, 31

- Dickinson, M., Papovich, C., Ferguson, H. C., & Budavári, T. 2003, *ApJ*, 587, 25
- Elbaz, D., Daddi, E., Le Borgne, D., et al. 2007, *A&A*, 468, 33
- Elbaz, D., Hwang, H. S., Magnelli, B., et al. 2010, *A&A*, 518, L29
- Elbaz, D., Dickinson, M., Hwang, H. S., et al. 2011, *A&A*, 533, A119
- Elmegreen, D. M., Elmegreen, B. G., Ravindranath, S., & Coe, D. A. 2007, *ApJ*, 658, 763
- Förster Schreiber, N. M., Genzel, R., Bouché, N., et al. 2009, *ApJ*, 706, 1364
- Geach, J. E., Smail, I., Moran, S. M., et al. 2011, *ApJ*, 730, L19
- Gilli, R., Comastri, A., & Hasinger, G. 2007, *A&A*, 463, 79
- Häring, N., & Rix, H.-W. 2004, *ApJ*, 604, L89
- Hopkins, P. F., & Hernquist, L. 2009, *ApJ*, 698, 1550
- Hopkins, P. F., Richards, G. T., & Hernquist, L. 2007, *ApJ*, 654, 731
- Jahnke, K., Bongiorno, A., Brusa, M., et al. 2009, *ApJ*, 706, L215
- Karim, A., Schinnerer, E., Martínez-Sansigre, A., et al. 2011, *ApJ*, 730, 61
- Kartaltepe, J. S., Dickinson, M., Alexander, D. M., et al. 2011, *arXiv:1110.4057*
- Kocevski, D. D., Faber, S. M., Mozena, M., et al. 2012, *ApJ*, 744, 148
- Kormendy, J., Bender, R., & Cornell, M. E. 2011, *Nature*, 469, 374
- Luo, B., Bauer, F. E., Brandt, W. N., et al. 2008, *ApJS*, 179, 19
- Magnelli, B., Elbaz, D., Chary, R. R., et al. 2011, *A&A*, 528, A35
- Marconi, A., Risaliti, G., Gilli, R., et al. 2004, *MNRAS*, 351, 169
- Mullaney, J. R., Pannella, M., Daddi, E., et al. 2012, *MNRAS*, 419, 95
- Noeske, K. G., Weiner, B. J., Faber, S. M., et al. 2007, *ApJ*, 660, L43
- Pannella, M., Carilli, C. L., Daddi, E., et al. 2009, *ApJ*, 698, L116
- Ranalli, P., Comastri, A., & Setti, G. 2003, *A&A*, 399, 39
- Renzini, A. 2006, *ARA&A*, 44, 141
- Rodighiero, G., Daddi, E., Baronchelli, I., et al. 2011, *ApJ*, 739, L40
- Salmi, F., Daddi, E., Elbaz, D., et al. 2012, submitted to *ApJL*
- Santini, P., Rosario, D., Shao, L., et al. 2012, *ArXiv e-prints*
- Sargent, M. T., Béthermin, M., Daddi, E., & Elbaz, D. 2012, *ApJ*, 747, L31
- Schawinski, K., Treister, E., Urry, C. M., et al. 2011, *ApJ*, 727, L31
- Shen, Y., Greene, J. E., Strauss, M. A., Richards, G. T., & Schneider, D. P. 2008, *ApJ*, 680, 169
- Silverman, J. D., Lamareille, F., Maier, C., et al. 2009, *ApJ*, 696, 396
- Tacconi, L. J., Genzel, R., Neri, R., et al. 2010, *Nature*, 463, 781
- Targett, T. A., Dunlop, J. S., & McLure, R. J. 2012, *MNRAS*, 420, 3621
- Vasudevan, R. V., & Fabian, A. C. 2007, *MNRAS*, 381, 1235
- Vattakunnel, S., Tozzi, P., Matteucci, F., et al. 2012, *MNRAS*, 420, 2190
- Volonteri, M., & Stark, D. P. 2011, *MNRAS*, 417, 2085
- Xue, Y. Q., Luo, B., Brandt, W. N., et al. 2011, *ApJS*, 195, 10